Integrated design of a gas separation system for the upgrade of crude SNG with membranes

Martin Gassner[a], Renato Baciocchi[b,c], François Maréchal[a], Marco Mazzotti[b]

[a]Laboratory for Industrial Energy Systems, Ecole Polytechnique Fédérale de Lausanne
CH – 1015 Lausanne, Switzerland
[b]Separation Processes Laboratory, Eidgenössische Technische Hochschule Zürich
CH – 8092 Zürich, Switzerland
[c]Department of Civil Engineering, University of Rome "Tor Vergata"
I – 00133 Rome, Italy

Chemical Engineering and Processing (2009), in press, doi:10.1016/j.cep.2009.07.002

Abstract

This paper investigates different design strategies and process layouts for upgrading crude synthetic natural gas (SNG) produced from lignocellulosic biomass to grid quality. The design problem is outlined by studying the involved key aspects with respect to the crude composition, purity requirements and process integration. A discussion of candidate technology identifies multistage membrane processes as a promising option, for which a multicomponent thermo-economic design model is coupled to a process model for SNG production. In a design study using multi-objective optimisation, the most promising membrane configurations are identified and optimised with respect to cost and efficiency. Comparing design strategies that consider different levels of process integration, it is shown that coupling the reactive and separation sections improves the process design. If process integration is not considered, the separation system is oversized by up to 60% and its investment cost is up to 46% too high. In the last part of the paper, the by-production of biogenic CO_2 at sufficient purity for storage is investigated, which would turn the process into a CO_2-sink for the atmosphere. The cost of captured CO_2 is assessed between 15 and 40 €/ton, which makes it potentially more advantageous than the capture at a fossil fuel power plant.

Keywords: SNG, gas separation, membranes, modelling, process integration, carbon capture

Nomenclature

Abbreviations

CC	Countercurrent
CCS	Carbon capture and storage
CMS	Carbon molecular sieves
EOR	Enhanced oil recovery
FICFB	Fast internally circulating fluidised bed
PSA	Pressure swing adsorption
rec	recycle
SNG	Synthetic natural gas
TSA	Temperature swing adsorption

Roman letters

A	Membrane area	m^2
C_I	Investment cost	€
$C_{I,d}$	Discounted investment cost	€/MWh_{SNG}

C_M	Maintenance cost	€/MWh$_{SNG}$
C_{OL}	Operating labour cost	€/MWh$_{SNG}$
C_P	Production cost	€/MWh$_{SNG}$
C_{RM}	Raw materials' cost	€/MWh$_{SNG}$
C_{UT}	Utility cost	€/MWh$_{SNG}$
$\tilde{c}$	Molar fraction	%
C_i	Cost or price of i	€ or €/MWh$_i$
$\dot{E}$	Mechanical or electrical power	kW
e_{spec}	Specific power consumption	kW$_{el}$/MW$_{th}$
i_r	Interest rate	%
$\dot{m}$	Mass flow	kg/s
n	Discount period	years
$\dot{n}$	Molar flow	kmol/s
p	Pressure	bar
P_a	Yearly production	MWh$_{SNG}$/year
P	Permeability	barrer
p_m	Methanation pressure	bar
$p_{s,p}$	Steam production pressure	bar
$\dot{Q}$	Heat	kW
R	Dimensionless permeation factor/area	-
r_{SNG}	SNG recovery in separation	%
$s_{in,2}$	Fraction of membrane inlet to stage 2	-
$s_{p1,E1}$	Fraction of permeate 1 to stage E1	-
T_m	Methanation temperature	K
$T_{s,s}$	Steam superheat temperature	K
$T_{s,u2}$	Steam utilisation level 2	K
Greek letters		
α	Selectivity	-
δ	Thickness of membrane layer	Å
$\Delta\tilde{h}_r^0$	Standard heat of reaction	kJ/mol
Δh^0	Lower heating value	kJ/kg
ε	Energy efficiency	%
Φ_{wood}	Wood humidity	%wt
Π_r	Pressure ratio	-
θ	Molar stage cut	-
Subscripts		
$_{el}$	electric	
$_f$	feed	
$_p$	permeate	
$_r$	retentate	
$_{th}$	thermal	
Superscripts		
^{0}	Standard conditions (298K, ideal gas)	
$^+$	Material or energy stream entering the system	
$^-$	Material or energy stream leaving the system	
^{sep}	Separation system	

1 Introduction

The production of fuels from biomass and waste is considered as an important contribution for mitigating climate change by reducing greenhouse gas emissions. Contrary to biological processes like biometha-

nation or ethanol fermentation, thermochemical processes allow for a complete conversion of lignocellulosic materials by gasification. Among the candidate liquid and gaseous synthetic fuels, methane is one of the most promising options since the synthesis reaction approaches chemical equilibrium and its conversion efficiency is high and less exothermic than the one of liquid fuel. Distributed as synthetic natural gas (SNG) in the existing natural gas grid, it can be used as transport fuel in an increasingly dense network of fuel stations.

While several recent studies have investigated suitable technology and processes for SNG production (Mozaffarian and Zwart, 2003; Duret et al., 2005; Gassner and Maréchal, 2009b; Heyne et al., 2008; Luterbacher et al., 2009; Gassner and Maréchal, 2009c), the issue of the gas upgrading to grid quality has not received much attention. The separation of carbon dioxide from methane is considered as a conventional operation in the removal of sour gas from natural gas in petrochemical applications, and relatively mature technology for the upgrade of biogas is available (Urban et al., 2008). For SNG production, different candidate technologies have been identified and some basic performance data and simple phenomenological models have been reported for physical absorption (Mozaffarian and Zwart, 2003; Gassner and Maréchal, 2009b), chemical adsorption (Heyne et al., 2008), membrane permeation (Duret et al., 2005) and pressure swing adsorption (PSA) (Gassner and Maréchal, 2009b). However, the detailed design of such a system needs to adapt not only to the quality and impurities of the crude product, but can also exploit the advantages of process integration. The present paper therefore investigates different design strategies for upgrading crude SNG to grid quality. Through the example of gas separation with membranes, it aims at showing in particular the benefits of a holistic design approach that considers a tight integration of the separation system with the reactive sections of the process. A suitable thermo-economic model of the membrane system is presented and coupled to a process model for crude SNG production. Multi-objective optimisation is used to compare different design approaches and optimal system layouts, and operating conditions for processes with and without CO_2-capture are proposed.

2 Process design problem

2.1 Production of crude SNG

Representing lignocellulosic biomass as a chemical molecule with the carbon atom as reference, the conceptual design of its conversion into methane is based on reaction (1):

$$CH_{1.35}O_{0.63} + 0.3475\, H_2O \longrightarrow \\ 0.51125\, CH_4 + 0.48875\, CO_2,\ \Delta\tilde{h}_r^0 = -10.5 kJmol_{wood}^{-1} \quad (1)$$

Technically, the currently preferred route is to carry out the conversion in two reactive steps. As depicted on Figure 1, the production of SNG from lignocellulosic biomass consists in gasifying the biomass and converting the producer gas into methane. Prior to gasification, the raw material is dried to below 20-25%wt humidity in order to prevent excessive losses due to water evaporation. Due to the presence of dust, tars and catalyst poisons like sulphur compounds, the producer gas is then cleaned before entering the methane synthesis. The producer gas is then converted to methane in a catalytic fluidised bed reactor operated at 300-400°C and requires upgrading before being fed to the grid. A comprehensive description and comparison of the different technological options for gasification and methanation are given by Mozaffarian and Zwart (2003). From the current state of research and process development (Stucki, 2005), it is expected that the first installations will be based on indirectly heated fluidised bed gasification technology of FICFB-type that has been developed and commercialised by Hofbauer et al. (2002).

Using a detailed process model developed in previous research (Duret et al., 2005; Gassner and Maréchal, 2009b), expected gas compositions of the producer gas and the crude methanation product for this technology are reported in Table 1. The corresponding properties of the feed and the process conditions considered for this base case are given in Tables 2 and 3, respectively. Depending on the operating conditions of the methanation reactor, cold, crude SNG contains around 50%vol of methane and 45%vol

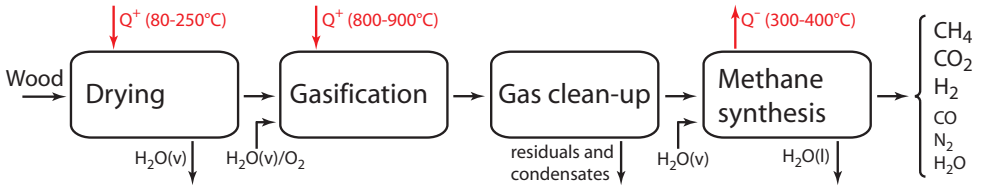

Figure 1: Block flow diagram of crude SNG production from wood.

		C_2H_4	CH_4	H_2	CO	CO_2	N_2	H_2O
Gasification	hot	1.9	9.2	32.8	21.5	15.7	0.4	18.5
(FICFB, 1123 K)	cold	2.2	10.9	38.8	25.5	18.6	0.5	3.5
Methanation	hot	-	26.7	3.6	0.1	27.1	0.6	41.9
(1 bar, 593 K)	cold	-	44.8	5.9	0.1	45.1	1.0	3.1
Methanation	hot	-	27.6	1.2	0.0	26.9	0.6	43.7
(10 bar, 593 K)	cold	-	52.1	1.7	0.0	44.7	1.2	0.3

Table 1: Composition of producer gas and crude SNG as calculated by the process model (%vol).

carbon dioxide. Especially at low pressure where the conversion is limited by thermodynamic equilibrium, a non-negligible residue of hydrogen and traces of carbon monoxide remain in the gas. According to Rauch (written around 2004), up to 5%vol[1] of nitrogen is furthermore present in the producer gas due to its use for the inertisation of the gasification feed and some slip from the adjacent combustion chamber. Since the methanation reaction reduces the volume of the reactants, the molar fraction of the inert species increases, which would prevent to meet the grid specifications for SNG without a special removal of nitrogen. In this work, it is assumed that this issue can be resolved by using CO_2 for feed inertisation and taking special care of nitrogen in an improved gasifier design, which allows for attaining a nitrogen content of 0.5%vol in the dry producer gas.

The stoichiometric design equation (Eq. 1) shows that the overall conversion of wood to methane is exothermic and releases about 450 kJ/kg_{wood} of heat. The block flow diagram (Fig. 1) illustrates, however, that this net release is distributed over the gasification and methanation reactions. The first one is endothermic and requires heat at high temperature, whereas the second one is exothermic and releases heat at lower temperature. The process thus requires additional energy and the quality of the process integration will define the overall process efficiency. The grand composite curve of the process streams shown in Figure 2 highlights that the process is pinched at the gasification temperature and that 200 - 250 kW of high temperature heat at 850 - 900°C are typically required to convert 1 MW[2] of wood to crude SNG.

2.2 Gas grid specifications

According to the new Swiss directive for the supply of biogas (also applying to synthetically produced gas) to the natural gas grid, unlimited amounts of gas can be fed in if its methane content is higher than 96%vol and the CO_2, H_2 and CO content less than 6, 4 and 0.5%vol, respectively (SVGW, 2008). Among other conditions, it is furthermore required that the dew point of the gas at grid pressure ($\leq$ 70 bar) is lower than -8°C. The limit with respect to methane content is thereby based on the fact that biogas as a binary mixture of methane and carbon dioxide does not meet a Wobbe index between 13.3 and 15.7 kWh/Nm^3 if its methane content is below 96%vol, which is the usual norm for H-quality natural gas.

[1] From the given composition, a typical value of 2.9%vol is computed by difference.

[2] based on the lower heating value of dry wood

Proximate analysis		Ultimate analysis	
$\Delta h^0_{wood,dry}$ [a]	18.6 MJ/kg$_{dry}$	C	51.09 %wt
Φ_{wood}	50.0 %wt	H	5.75 %wt
		O	42.97 %wt
		N	0.19 %wt

[a] Δh^0 is defined on dry basis, and thus independent of the humidity.

Table 2: Proximate and ultimate analysis of the feedstock.

Section	Operating conditions	Value
Drying	Inlet temperature	473 K
	Outlet wood humidity	20%wt
Gasification	Pressure	1 bar
	Gasification temperature	1123 K
	Steam preheat temperature	573 K
	Steam/dry biomass ratio	0.5
Methanation	Pressure	1 bar
	Inlet temperature	593 K
	Outlet temperature	593 K

Table 3: Nominal operating conditions of the process.

2.3 Design problem definition

Table 4 compares the obtained gas compositions after methanation with the grid specifications. Assuming that nitrogen can not be separated from methane, it shows the maximum obtainable purities after complete removal of water, carbon dioxide and hydrogen. Although a cut-down of the nitrogen fraction in the producer gas to 0.5%vol is considered feasible, it is not sufficient to remove only the carbon dioxide. Provided that an ideal separation process for removing CO_2 from the SNG is used, the hydrogen concentration of the SNG is expected to rise to around 3-11%, depending on the methanation conditions. The CH_4 purity will be at best around 94%, and at least some of the unconverted hydrogen must be removed. Apart from the separation of the bulk species, the table also shows that the residual carbon monoxide might be an issue. While for pressurised methanation, its fraction in the concentrated methane is at 0.1%vol, it approaches the directive's limit in case of a reactor at atmospheric pressure.

The identification of the minimum energy requirements of the process furthermore adds a supplementary aspect to the design problem. Gasification has a relatively important heat demand at high temperature, which is usually supplied by burning producer gas. In the combined heat and power application for which the gasification technology has originally been developed, few other fuel alternatives are available. However, in an SNG plant that necessarily suffers from a non-ideal separation, depleted gas streams from the SNG upgrading section could be used instead of the intermediate product. The condition for this is that its flame temperature is sufficiently higher than the gasification temperature. If the depleted gas is too diluted, it must in any case be treated in a catalytic combustion to eliminate the residual methane due

	C_2H_4	CH_4	H_2	CO	CO_2	N_2	H_2O
Methanation (1 bar, 593 K)	-	44.8	5.9	0.1	45.1	1.0	3.1
– without H_2O, CO_2	-	86.4	11.3	0.3	-	2.0	-
– without H_2O, CO_2, H_2	-	97.4	-	0.3	-	2.3	-
Methanation (10 bar, 593 K)	-	52.1	1.7	0.0	44.7	1.2	0.3
– without H_2O, CO_2	-	94.7	3.0	0.1	-	2.2	-
– without H_2O, CO_2, H_2	-	97.6	-	0.1	-	2.3	-
grid specifications		> 96	< 4	< 0.5		< 6	265 K

Table 4: Gas upgrading requirements (%vol).

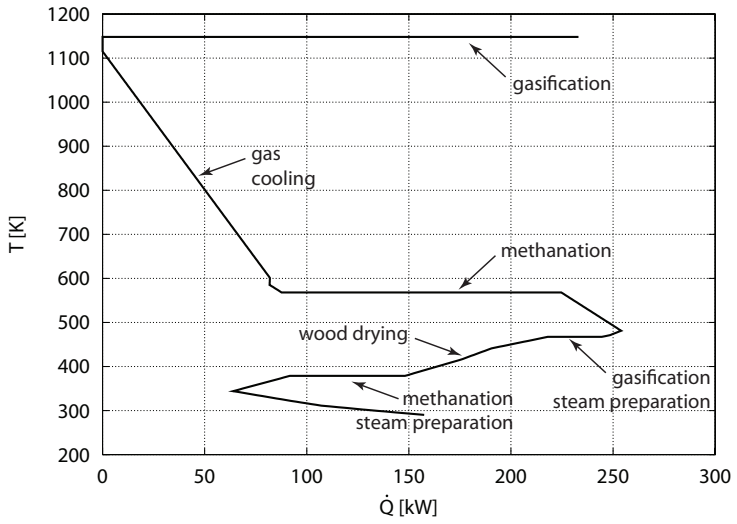

Figure 2: Grand composite curve of the minimum energy requirement normalised for the conversion of 1 MW of wood.

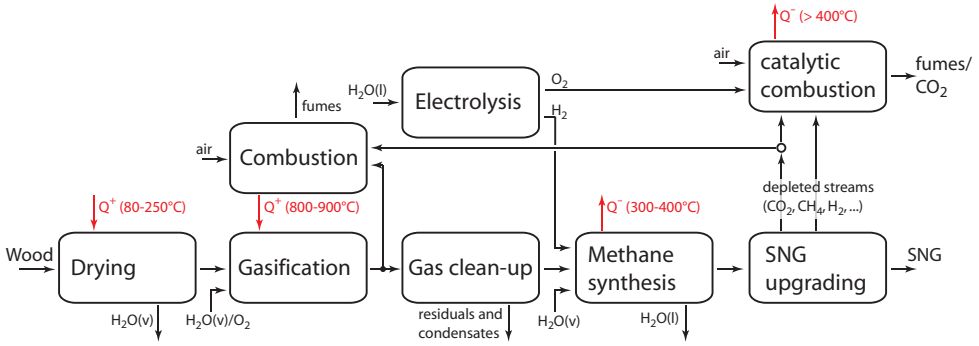

Figure 3: Block flow diagram of process integration options for SNG upgrading.

to its high environmental impact as a greenhouse gas.

From these considerations, it is obvious that the design of the separation system is not a trivial problem. It requires the development of an appropriate multicomponent separation system including drying, while also considering possible cost and energy savings originating from the trade-off between using the producer gas or a depleted gas as hot utility. In the framework of the actions aimed at climate change mitigation, rather pure carbon dioxide (95% minimum) may also represent a valuable by-product. In a near future, carbon dioxide storage sites are expected to be developed, and carbon dioxide could be transported to the storage sites through dedicated pipelines (Meth et al., 2005). If sequestration instead of venting the separated carbon dioxide is targeted, care must be taken not to dilute this by-product with nitrogen from combustion with air. A possible option is thereby to use oxygen produced by electrolysis in the catalytic combustion. As already discussed in (Gassner and Maréchal, 2008), the additional hydrogen could be supplied to the methane synthesis and would increase the SNG output since the producer gas lacks hydrogen to be completely reformed into methane. A general block flow diagram of these different upgrading options is given on Figure 3.

3 Candidate technologies for SNG upgrading

The required SNG specification can be achieved by applying one or more separation steps based on one of the following process options: physical or chemical absorption, membrane separation and adsorption separation. Although the choice of the most effective separation train is the result of a detailed optimisation effort, some general considerations can be proposed in order to obtain at least a preliminary selection of the suitable separation processes to be further investigated.

Natural gas must be dehydrated before transmission over a long distance through a pipeline to prevent the condensation of water. Indeed, liquids can reduce the volumetric capacity of the system and interfere with the operation of pressure regulators and filters. Furthermore, condensed liquids accumulated in pipelines cause an increase in the operating pressures (Gandhidasan, 2003). Water is removed from the gas to meet the water dew point requirements of the pipeline conditions. Three types of dehydration equipment are in current use: absorption by liquid desiccants (Gandhidasan, 2003), adsorption by solid desiccants (Gandhidasan et al., 2001) and membrane separation (Liu et al., 2001).

The operating conditions of the bulk CH_4/CO_2 separation from the SNG resemble those encountered in carbon dioxide enhanced oil recovery (EOR). In EOR fields, CO_2 is pumped underground at high pressure, where it arrives at the well and starts contaminating the natural gas associated with the well. This means that the gas collected from the well is a CH_4/CO_2 mixture with a CO_2 concentration that can raise up to values between 40 and 90% (Spillman, 1989). This mixture needs to be separated to obtain pure natural gas and pure CO_2 for reinjection. Since high injection pressure is needed, the separation process should be tailored to obtain a CO_2 stream at the highest possible pressure. Membrane separation has been proposed as a viable technology, since it may deal with feed streams at high CO_2 concentrations and pressures. Commercial cellulose acetate CO_2 selective membranes with a typical selectivity between CO_2 and CH_4 of 21 allow to achieve high CO_2 purity in the permeate stream (Bhide and Stern, 1993a,b). High CH_4 purity in the retentate can also be achieved, provided that a proper multistage scheme is used. Several configurations have been studied in the literature (Qi and Henson, 1998). It has been shown that in order to achieve high purity of both CH_4 and CO_2, the best configurations are the ones consisting of three stages with residue and/or permeate recycle (Bhide and Stern, 1993a). A cost comparison between this membrane process configuration and chemical absorption with ammine shows that the costs of gas absorption increase linearly with the CO_2 concentration in the feed (Bhide and Stern, 1993b). The gap between the two processes increases as well, making membrane process competitive at least at the operating pressure of 55 bar and with a 11.5 Nm^3/s feed flowrate. As expected, an increase of the operating pressure has a dramatic reducing effect on the cost of the membrane process, whereas it leads to a slight cost increase for the absorption process. For an operating pressure of 28 bar, the cost of the two processes are very close indeed, whereas the difference increases with increasing operating pressure (Bhide and Stern, 1993b).

Since cost of membrane separation is expected to rise when applied to feeds at lower operating pressure, and methane cost is already much higher now than at the time of the papers discussed above, membrane separation (with cellulose acetate) could lose its competitive advantage with respect to absorption for CO_2/CH_4 separation, unless a more selective membrane is used. A two-fold increase in selectivity (from the value of 21 of cellulose acetate, calculated for ideal conditions, i.e. no plasticisation) could lead to a 30% reduction of separation cost. Unfortunately, for polymeric materials, a rather general trade-off exists between permeability and selectivity, the so-called Robeson's upper bound (Robeson, 1991). High selectivity is needed to achieve a high purity product, while high permeability is desired to minimise membrane area and thus the capital cost. Materials that perform close to the upper bound in separation of simple gases are generally glassy polymers, such as polyimide, that typically show mobility selectivity, with smaller gas molecules diffusing more rapidly than larger ones (Cecopieri-Gomez et al., 2007) and polymers of intrinsic microporosity, which behave essentially like microporous materials (pores of effective size $<$2nm) (Budd et al., 2005). In order to enhance separation and avoid plasticisation, many researchers have focused on cross-linking modifications of polymeric membranes (Cao et al., 2003; Staudt-Bickel and Koros, 1999; Koros and Mahajan, 2000). A completely different alternative is provided by inorganic materials: zeolites, as SAPO-34 (Li et al., 2005), carbon molecular

sieves (Ismail and David, 2001; Hagg et al., 2003), mixed matrix membranes (Chung et al., 2007) and facilitated transport membranes (Zou and Ho, 2006) may provide a way of overcoming the Robeson's upper bound, although most of them are still not ready for commercial application, due to low stability under real operating conditions or simply to their cost (Baker, 2002).

Adsorptive separations may also represent an effective tool for addressing the issue of separating a CH_4/CO_2 stream for obtaining a pure CH_4 stream and in the meantime producing a high purity CO_2 stream. The main commercial suitable adsorbents rely either on the equilibrium selectivity (zeolites 5A and 13X) or on diffusion/kinetic selectivity (carbon molecular sieves, CMS). In both cases the most retained compound (heavy product) is CO_2, whereas the less retained one (light product) is CH_4. The CH_4/CO_2 bulk separation has been investigated using different pressure swing adsorption (PSA) cycles. A PSA Skarstrom cycle using CMS has been used for the separation of a 50/50 feed mixture, at operating pressures between 2 and 0.4 bar, achieving a purity of 91% in both product streams (Kapoor and Yang, 1989). The Skarstrom cycle was also applied to the ternary $CH_4/CO_2/N_2$ (60/20/20%) separation in a layered bed packed with zeolite 13X and CMS (Cavenati et al., 2006). The high pressure step was performed at up to 2.5 bar, and the low pressure at 0.1 bar; two temperatures were studied, namely 300 and 323K. The ratio of zeolite 13X to CMS was varied as well, in order to investigate its effect on performance. The results showed rather low CH_4 purity and recovery values, namely 73-85% and 88-27% respectively. Comparison of CMS PSA with the zeolite process showed that the former yields higher purity CH_4 product with improved recovery and also a larger amount of feed gas (feed/h/kg desorbent) treated (Kapoor and Yang, 1989). A slightly modified Skarstrom cycle with two equalisation steps, proposed by Kim et al. (2006) for a 50/50 CH_4/CO_2 feed and performed on a CMS bed, allowed to achieve a 95.8% CH_4 purity with a 71.2% recovery for operating pressures between 0.4 MPa and atmospheric pressure. Sircar (1988) proposed a five-step PSA cycle for the CH_4/CO_2 bulk separation, placed between a temperature swing adsorption (TSA) unit for moisture removal, and a second PSA for the separation of impurities. The purities of the products obtained, using zeolite 13X as adsorbent, were 99% for each species and the corresponding recoveries were of about 98 and 99% for CH_4 and CO_2, respectively. A detailed comparison between PSA and membrane systems for the bulk separation discussed here does not exist in the literature. Some authors have attempted comparing purities and recoveries of the two processes based on similar (but not equal) problems using data from the literature (Kapoor and Yang, 1989). From this analysis, the two processes look similar in terms of process performance, although the feed pressure required in the membrane process was 10 times higher. Further purification of the SNG stream depends upon the separation process applied for CO_2/CH_4 separation. H_2/CH_4 and N_2/CH_4 separation could be performed by either PSA (Knaebel and Reinhold, 2003; Waldron and Sircar, 2000; Doong and Yang, 1987) or membrane separation (Hradil et al., 2004; Adhikari and Fernando, 2006; Ritter and Ebner, 2007).

4 Thermo-economic modelling

4.1 Process modelling

In previous work, a thermo-economic process model for the production of SNG from wood has been developed and reconciled with experimental data (Duret et al., 2005; Gassner and Maréchal, 2009b). According to the applied design methodology (Gassner and Maréchal, 2009a), its thermodynamic part is divided into an energy-flow and an energy-integration model. In the energy-flow model, the thermodynamic conversions occurring in the different process units are modelled with a commercial flowsheeting tool (Belsim SA, last visited 04/2009). The heat requirements of the process units are transferred to the energy-integration model, where the energy conversion and heat transfer system is determined by a mixed integer linear programming model targeting minimum operating costs with respect to the minimum approach temperature constraints. The thermodynamic conditions are then considered as design targets for the process equipment, which is rated and costed by design heuristics from Ulrich and Vasudevan (2004), Turton et al. (1998) and data from existing experimental and pilot plant facilities.

In order to investigate the impact of process integration on the optimal design of the separation system and the reactive sections of the plant, multi-stage membrane separation has been chosen among the identified candidate technologies for a detailed modelling. Preliminary to the simultaneous bulk separation of CH_4, H_2 and CO_2, gas drying in a TSA unit with an activated alumina adsorbent is considered, which allows for attaining a dew point of -70°C with a heat consumption of 11 MJ/kg_{H2O} for regeneration at 160-190°C (Bart and von Gemmingen, 2009).

4.2 Unit models for membrane separation

According to the theory of gas separation by membranes, a practical description of the permeation process through a membrane has to consider the difference of partial pressure in the bulk as driving force (Hwang and Kammermeyer, 1975). Using a phenomenological constant termed permeability P_i, the permeation of species i is described as:

$$\frac{d\dot{n}_{i,p}}{dA} = \frac{P_i}{\delta}\,(p_{i,r} - p_{i,p}) \tag{2}$$

where $\dot{n}_{i,p}$ is the partial molar flow of i that permeates the membrane, A the membrane area, δ its thickness, and $p_{i,r}$ and $p_{i,p}$ the partial pressure of species i on the retentate and permeate side, respectively. The permeability P_i is thereby often given in barrer [$cm^2s^{-1}cmHg^{-1}$], which corresponds to $7.5005 \cdot 10^{-18}$ [$m^2s^{-1}Pa^{-1}$] in SI-units. Furthermore, it is convenient to specify the relative permeabilities of two different species i and j by the selectivity $\alpha_{i,j}$ of i over j:

$$\alpha_{i,j} = P_i/P_j \tag{3}$$

As the permeation is described by a set of i differential equations of the same type as Eq. 2, its resolution depends on the flow pattern of the membrane. Typical patterns discussed in the literature, for example by Hwang and Kammermeyer (1975) or Rautenbach and Dahm (1985), are the completely mixed, cross-flow (also termed plug-flow) and parallel flow (either co- or counter-current) types and apply to plate and frame, spiral wound and hollow fibre modules, respectively. Analytic solutions for these different flow schemes have been developed in pioneering work by mainly Weller and Steiner (1950) for binary mixtures and are comprehensively compared by Hwang and Kammermeyer (1975). For multicomponent systems no analytic solutions have been reported, but some simplified analytic or numeric procedures are suggested. Hogsett and Mazur (1983) present a simplified design approach for spiral wound membranes, in which fast and slow permeating gases are lumped together and a log-mean average of the feed and retentate streams is claimed to be empirically accurate enough to determine the partial pressure on the rich side. Rautenbach and Dahm (1985) doubt on the accuracy of this approach and present advanced iterative procedures for all flow patterns. However, such an approach is impractical for flowsheet calculations since it lacks numerical robustness. For this reason, Pettersen and Lien (1994) developed and validated a simplified algebraic design model for hollow-fibre modules in counter-current operation, where the analogy to heat exchangers is exploited. As detailed in Appendix A, the permeate molar fraction $\tilde{c}_{i,p}$ of a substance i is thereby explicitly calculated from its feed fraction $\tilde{c}_{i,f}$ and design parameters like the pressure ratio Π_r, the molar stage cut θ and a dimensionless permeation factor R_i, which is also interpreted as a dimensionless area of the membrane.

In order to compare the quality of the separation for the different flow schemes, the characteristics of a single membrane stage are computed for a typical binary biogas mixture of 60/40% CH_4/CO_2. The selected material is cellulose acetate, which is a commercial membrane used for the removal of CO_2 from natural gas and in enhanced oil recovery (Bhide and Stern, 1993a). Typical properties of such membranes, which are available as spiral wound or hollow fibre modules, are given in Table 5. As shown in Figure 4, considerable differences occur between a completely mixed and the more advanced cross- and countercurrent flow patterns. Especially for stage cuts between 0.2 and 0.6 which provide a reasonable trade-off between purity and recovery, completely mixed modules suffer from the continuous dilution of the retentate with fresh feed. The obtained CH_4-purity is up to 10% lower than in the other

P_{CO2}	9.00 barrer	δ	1000 Å
P_{H2}	2.63 barrer		
P_{CH4}, P_{CO}, P_{N2}	0.426 barrer		

Table 5: Properties of cellulose acetate membranes (Bhide and Stern, 1993a; Phair and Badwal, 2006).

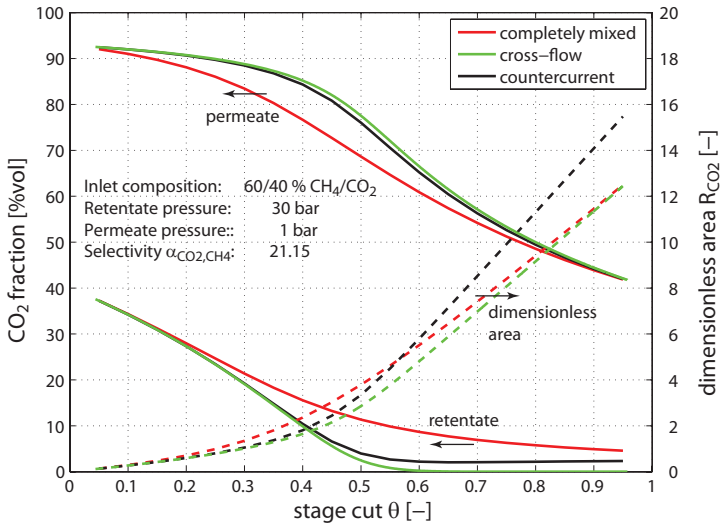

Figure 4: Single-stage performance of different membrane unit models.

cases, and more membrane area is required for a worse separation. The performances of the cross- and countercurrent modules are very similar. Small differences occur only at very high cut rates which are not interesting in practice since not only the fast species but also a large amount of the slow one permeates the membrane. In this domain, the countercurrent retentate contains some residual CO_2 since a log-mean average for its partial pressure across the membrane is used. In a cross-flow scheme, the fast permeator completely diffuses through the module due to the assumption that it is immediately swept away from the membrane surface on the permeate side.

4.3 Flowsheet options

In principle, the most general operational scheme of a membrane system is a network of membranes where the permeate and retentate streams of each module can connect to the inlet of all other membranes or mix to the CH_4- or CO_2-rich outlet. All these modules can operate at different feed and permeate pressures, and the most general network definition includes a stream conditioning unit for each connection. If the subsequent stage of an outlet stream is at higher pressure, it requires compression and cooling, while lower pressure allows for power recovery by a reheat and expansion stage. However, as it is generally not advantageous to remix priorly separated species, the membrane stages are typically arranged in cascades where the depleted streams are recycled to a preceding stage of lower purity. Although a systematic problem formulation with a superstructure model solved by mixed integer optimisation (like for example in Girardin et al. (2006)) could have been used, preliminary calculations with a typical biogas mixture of 60/40% CH_4/CO_2 for countercurrent cascades of 1 to 4 stages and simplified schemes with less recycle options have been conducted to better understand the system interactions. The three most promising configurations of the general superstructure depicted in Figure 5a for the considered membrane properties have been selected for the design study. They include a two-stage countercurrent cascade with the feed location on the CO_2-rich side of stage 1 (Fig. 5b), a three-stage countercurrent cascade with a splitted feed to the CO_2-rich stage 1 and the intermediate stage 2 (Fig. 5c), and a simplified three-stage scheme with a common recycle of the depleted permeate streams from the intermediate stage 2 and CH_4-side

stage 3 to the CO_2-rich stage 1 (Fig. 5d). In the preliminary calculations, not only the membrane system configuration, but also its integration in the production plant depicted in Figure 3 has been investigated. Especially when the separated streams are valuable products or recovered as combustibles to provide high temperature heat, the quality of the depleted stream(s) is important and depends on the location where it is withdrawn from the membrane system. If CO_2-capture is not considered, the first stage retentate has been identified as the most advantageous location for extracting the diluted mixture. If CO_2 is a valuable by-product, it is promising to withdraw it from the additional enriching stage E1 and use its retentate as fuel. It is further observed that gradually increasing the operating pressure from low to high CH_4-purity stages is advantageous since the gas grid pressure is at higher pressure than the crude gas. Power recovery by expansion of the gas is thus disregarded, and only compression stages of 80% isentropic efficiency are retained for the feed and recycling streams.

4.4 Economic model

In order to assess the economic performance of the system, the investment cost of the plant is estimated by rating all major equipment and using the costing method and correlation data from mainly Turton et al. (1998). According to this approach, the investment cost for the separation system is computed by factoring the cost contributions from the membranes and the compressors to account for other expenses associated with the construction of the plant. The purchase cost of the membranes is assessed by updating the cost data reported by Bhide and Stern (1993a), who considered an initial permeator module cost of 108 US\$/m^2 and a membrane element cost of 54 US\$/m^2 that needs replacement every 3 years. For the compressors, cost data from Turton et al. (1998) for centrifugal compressors and appropriate electric drives are used. The preceding two-column TSA unit for gas drying is sized by assuming a cycle time of 12 h and a maximum adsorbent loading of 0.12 $kg_{H2O}/kg_{adsorbent}$ (Ducreux et al., 2006). According to Ulrich and Vasudevan (2004), the cost of the adsorbent and its density have been assumed to 9 US\$/kg and 800 kg/m^3, respectively. Detailed sizing and costing information for all other process units of the biomass conversion process is reported in Gassner and Maréchal (2009b).

5 Design study

5.1 Approach

Following the previously mentioned design methodology (Gassner and Maréchal, 2009a), the process model is coupled to a multi-objective optimisation algorithm to assess the most promising membrane separation layouts, its operating conditions and the possible energy integration options. In order to highlight the influence of the design strategy, several process optimisations for fixed operating conditions of the crude SNG production are carried out. The flowsheets generated by the optimisation algorithm are then analysed with respect to different sets of performance indicators. A first set of indicators is chosen in order to represent the performance of the isolated separation system, while a second one assesses the performance of the integrated plant. Definitions of these sets are given in Section 5.2. Solutions that appear optimal with respect to the different sets of indicators are identified and compared to each other.

In addition to the comparison of the design approach and the assessment of the optimal set-up for basic SNG upgrading (Section 5.3), the model is explored for the design of a separation system that also produces CO_2 in adequate quality for sequestration (Section 5.4).

5.2 Performance indicators

In order to compare an isolated with a holistic design approach, different sets of thermo-economic indicators representing the performance of the separation system and the overall plant are required. In this work, the energetic performance of the membrane separation is assessed by its energy efficiency, defined

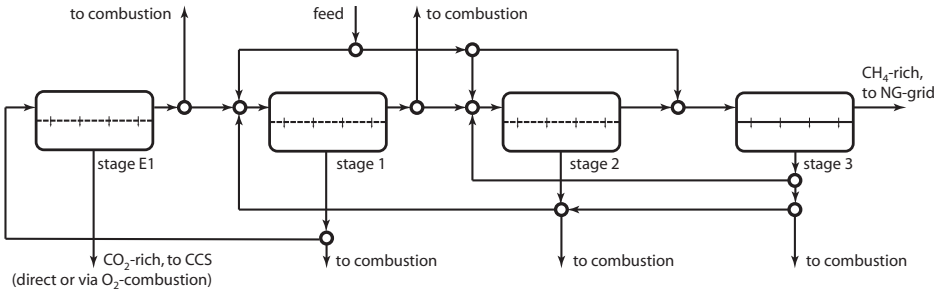

a - all investigated options of the membrane superstructure

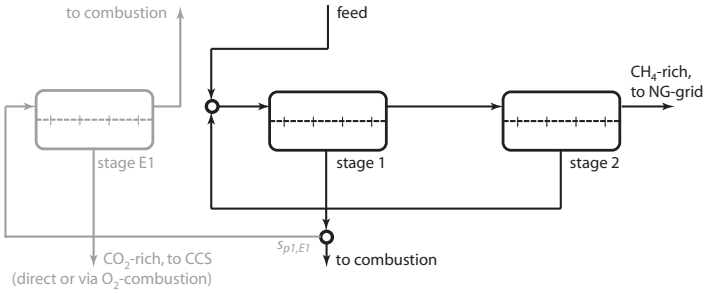

b - two-stage, countercurrent recycling

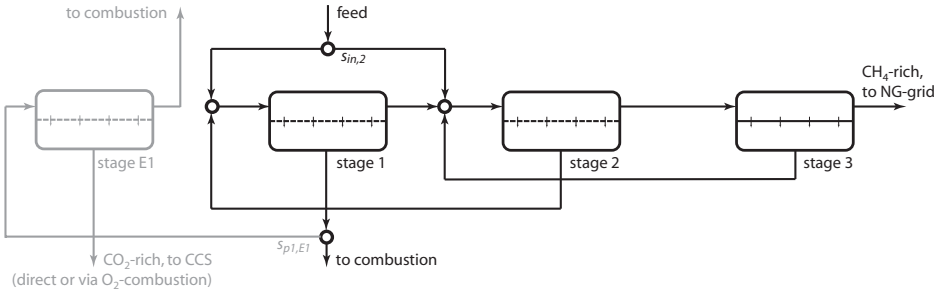

c - three-stage, countercurrent recycling

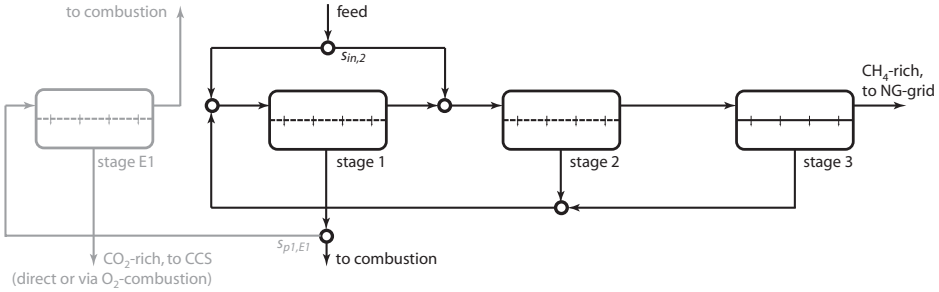

d - three-stage, one common recycle loop

Figure 5: All investigated and most promising layouts of the membrane system. The additional stage for CO_2-enrichment (E1, in grey) instead of combusting the permeate of stage 1 is only considered in Section 5.4.

as (Eq. 4):

$$\varepsilon^{sep} = \frac{\Delta h^0_{SNG} \dot{m}^-_{SNG}}{\Delta h^0_{crudeSNG} \dot{m}^+_{crudeSNG} + \dot{E}^{sep,+}} \tag{4}$$

where Δh^0 terms the heating value of the streams, $\dot{m}$ their mass flows and $\dot{E}^{sep}$ the electric power required for the separation. The superscripts '+' and '–' stand for quantities that enter and leave the system boundaries, respectively. As economic indicator, all the costs C_P related to the separation are considered. These costs include the investment and operating costs, i.e. the discounted investment $C_{I,d}$, maintenance costs C_M, expenses for utilities C_{UT} and a cost reflecting the loss of the raw materials' energy content in the depleted stream C_{RM} (Eq. 5):

$$C^{sep}_P = C^{sep}_{I,d} + C^{sep}_M + C^{sep}_{UT} + C^{sep}_{RM} \tag{5}$$

with

$$C^{sep}_{I,d} = \frac{(1+i_r)^n - 1}{i_r (1+i_r)^n} \frac{C^{sep}_I}{P_a} \tag{6}$$

$$C^{sep}_M = 0.05 \frac{C^{sep}_I}{P_a} \tag{7}$$

$$C^{sep}_{UT} = \frac{\dot{E}^{sep,+}}{\Delta h^0_{SNG} \dot{m}^-_{SNG}} C_{el} \tag{8}$$

$$C^{sep}_{RM} = \left(\Delta h^0_{crudeSNG} \dot{m}^+_{crudeSNG} - \Delta h^0_{SNG} \dot{m}^-_{SNG} \right) C_{SNG} \tag{9}$$

In these formulations, C_I stands for the initial investment, P_a for the yearly SNG production, i_r for the interest rate and n for the discount period of the plant. The yearly maintenance costs are supposed to amount to 5% of the initial investment. Prices for electricity and SNG are termed C_{el} and C_{SNG}.

In analogy with the definitions for the separation system, the energy efficiency ε of the overall process is used as indicator for its energetic performance. With the system limits of the entire plant, it becomes (Eq. 10):

$$\varepsilon = \frac{\Delta h^0_{SNG} \dot{m}^-_{SNG} + \dot{E}^-}{\Delta h^0_{wood,dry} \dot{m}^+_{wood,dry} + \dot{E}^+} \tag{10}$$

whereas the total electricity balance of the plant $\dot{E}$ only occurs either in the numerator or denominator of the equation. Compared to the cost of separation, the total production cost of SNG is completed by a term for operating labour C_{OL}, and the actual expenses for wood are used as cost for the raw material instead of accounting for the gas loss in the separation. With these changes, the total production cost sums up as (Eq. 11):

$$C_P = C_{I,d} + C_M + C_{OL} + C_{UT} + C_{RM} \tag{11}$$

with

$$C_{I,d} = \frac{(1+i_r)^n - 1}{i_r (1+i_r)^n} \frac{C_I}{P_a} \tag{12}$$

$$C_M = 0.05 \frac{C_I}{P_a} \tag{13}$$

$$C_{OL} = \frac{C_{salaries}}{P_a} \tag{14}$$

$$C_{UT} = \frac{\dot{E}^+}{\Delta h^0_{SNG} \dot{m}^-_{SNG}} C_{el} \tag{15}$$

$$C_{RM} = \frac{\Delta h^0_{wood} \dot{m}^+_{wood}}{\Delta h^0_{SNG} \dot{m}^-_{SNG}} C_{wood} \tag{16}$$

The parameters used in Equations 5 - 9 and 11 - 16 for the economic evaluation are given in Table 6.

Parameter	Value
Marshall&Swift index (2006)	1302
Dollar exchange rate	1 €/US$
Interest rate	6%
Discount period	15 years
Plant availability	90%
Operators[a]	4 p./shift
Operator salary	60 k€/year
Maintenance costs	5%/year of C_I
Wood price (Φ_{wood}=50%wt)	33.3 €/MWh
Electricity price	180 €/MWh
SNG price	120 €/MWh

[a] Full time operation requires three shifts per day. With a working time of five days per week and 48 weeks per year, one operator per shift corresponds to 4.56 employees.

Table 6: Assumptions for the economic analysis.

Operating conditions		Unit	2-stage	3-stage
Stage cut of stage 1	θ_1	-	[0.2 0.5]	[0.2 0.6]
Stage cut of stage 2	θ_2	-	-	[0.2 0.6]
Stage cut of stage E1[a]	θ_{E1}	-	[0.2 0.8]	[0.2 0.8]
Permeate pressure of stage 1	p_{p1}	bar	[1 5]	[1 5]
Permeate pressure of stage 2	p_{p2}	bar	[1 5]	[1 5]
Permeate pressure of stage 3	p_{p3}	bar	-	[1 5]
Permeate pressure of stage E1[a]	p_{pE1}	bar	[0.2 0.8]	[0.2 0.8]
Feed pressure of stage 1	p_{f1}	bar	[5 50]	[5 50]
Feed pressure of stage 2	p_{f2}	bar	[5 50]	[5 50]
Feed pressure of stage 3	p_{f3}	bar	-	[5 50]
Fraction of feed to stage 2	$s_{in,2}$	-	-	[0 1]
Fraction of permeate 1 to E1[a,b]	$s_{p1,E1}$	-	-	[0 1]

[a] CCS only (Section 5.4)

[b] direct capture only

Table 7: Decision variables of the membrane system.

5.3 Optimal design of the SNG upgrading system

The optimal design of the SNG upgrading system to 96%vol pure CH_4 is performed for fixed base case conditions of the crude gas production (Table 3). The decision variables are therefore chosen among the operating conditions of the membranes system. In all cases, they include the stage cuts of each stage but the last (CH_4-rich) one as well as the total pressure on the permeate and the feed sides. For the three-stage layouts, the fraction of the inlet stream that is fed to stage 2 is furthermore considered as a decision variable. The search space for all decision variables is given in Table 7.

The objective functions used in the mathematical problem formulation must allow for generating a complete set of optimal solutions with respect to the selected performance indicators. In the present case, maximising the SNG recovery r_{SNG} (Eq. 17) and minimising both the specific power consumption e_{spec}^{sep} (Eq. 18) and the investment cost of the separation system C_I^{sep} have proven to be adequate and efficient for this purpose:

$$r_{SNG} = \frac{\Delta h_{SNG}^0 \dot{m}_{SNG}^-}{\Delta h_{crudeSNG}^0 \dot{m}_{crudeSNG}^+} \quad (17)$$

$$e_{spec}^{sep} = \frac{\dot{E}^{sep,+}}{\Delta h_{crudeSNG}^0 \dot{m}_{crudeSNG}^+} \quad (18)$$

The numeric optimisation results are shown in Figure 6 as two-dimensional projections of the three-

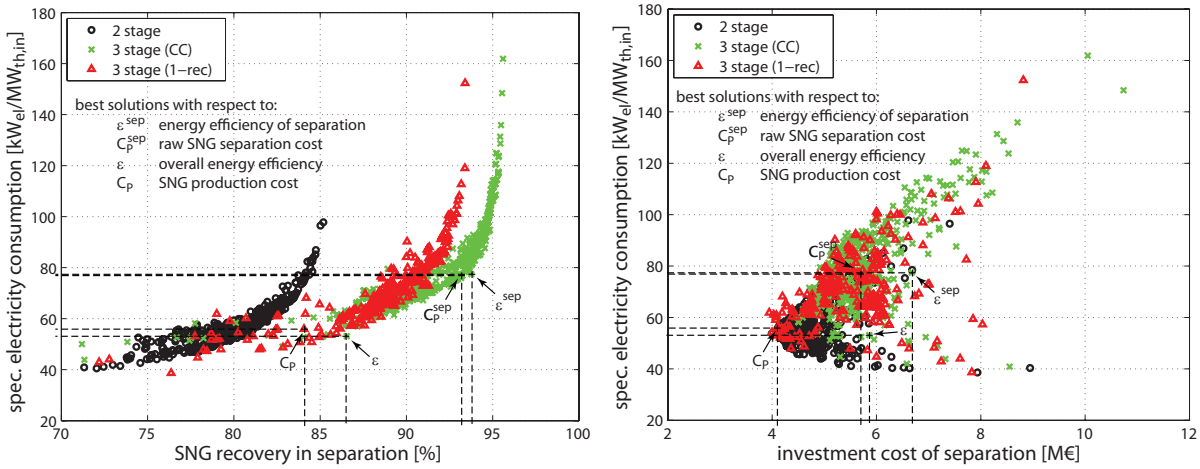

Figure 6: Projections of the Pareto-optimal solutions of the separation system: trade-off between SNG recovery and power consumption (left) and investment cost and power consumption (right).

dimensional objective space. The plots show that the SNG recovery and specific power consumption are clearly conflictive, whereas no general trend is observed for the investment cost. For high recovery ratios, the latter is positively correlated with the specific power consumption since it is dominated by the need for powerful compressors. For low recoveries, this trend is reversed by the increasing cost for larger membrane areas that are necessary to achieve higher stage cuts. Comparing the different layouts, it is observed that a two-stage system limits the SNG recovery to about 85%, while more than 95% are achievable with a countercurrent three-stage system. The limit of the alternative three-stage layout with one recycle is at about 93% recovery. However, for values above 90%, its specific power consumption is clearly higher than the one of the countercurrent scheme.

Figure 7 shows the thermo-economic performance indicators for the separation system ant the total process. Details of the optimal solutions with respect to energy efficiency and production cost are given in Tables 8 and 9, respectively. Considering the isolated performance of the separation system (plots and columns on the left), it is observed that all membrane layouts pass through an optimal value for the SNG recovery with respect to efficiency and cost. At low recovery levels, the performance suffers from elevated gas losses, whereas at high recoveries, the power consumption and cost of the compression get excessive. The two-stage scheme is clearly suboptimal due to its lowest recovery level. Although the three-stage systems are close for a large recovery range, the countercurrent scheme performs best since highest recoveries are attained. At values of 93.2% and 93.8%, it reaches a minimum separation cost and maximum efficiency of 32.4 €/MWh and 87.0%, respectively. Comparing the generated solutions with respect to the overall performances (plots and columns on the right), it is observed that the slope of the curves are flatter and that increasing the recovery above 85% does not have any beneficial effect. When considering the integrated system, both the operating conditions and system layout are changed. As indicated in Tables 8 and 9, the value of $s_{in,2}$ shows that the best feed location switches from stage 2 to 1. Rather than using a countercurrent scheme, the most efficient and economic solutions are obtained with the three-stage one-recycle layout at 83.8% and 84.1% SNG recovery, respectively. Implementing the optimal solution suggested by the analysis of the isolated performance of the separation system (i.e. a three-stage countercurrent scheme with 93.2-93.8% recovery) would thus lead to a suboptimal system solution. The data in the tables shows that the membrane area would be oversized by 58-60%, leading to investment costs that are 39-46% higher than for the global optimum.

These results clearly indicate that the depleted permeate stream is not lost and its quality is sufficient to be valuable as hot utility. As shown in Figure 8, it still contains a considerable amount of methane beneath the hydrogen that permeates very fast in the cellulose acetate membrane. The adiabatic flame temperature of the stream is therefore high enough to transfer heat to the gasification reactor, which is illustrated by the energy flow diagram depicted in Figure 9. At 95% recovery, 19.9% of the chemical

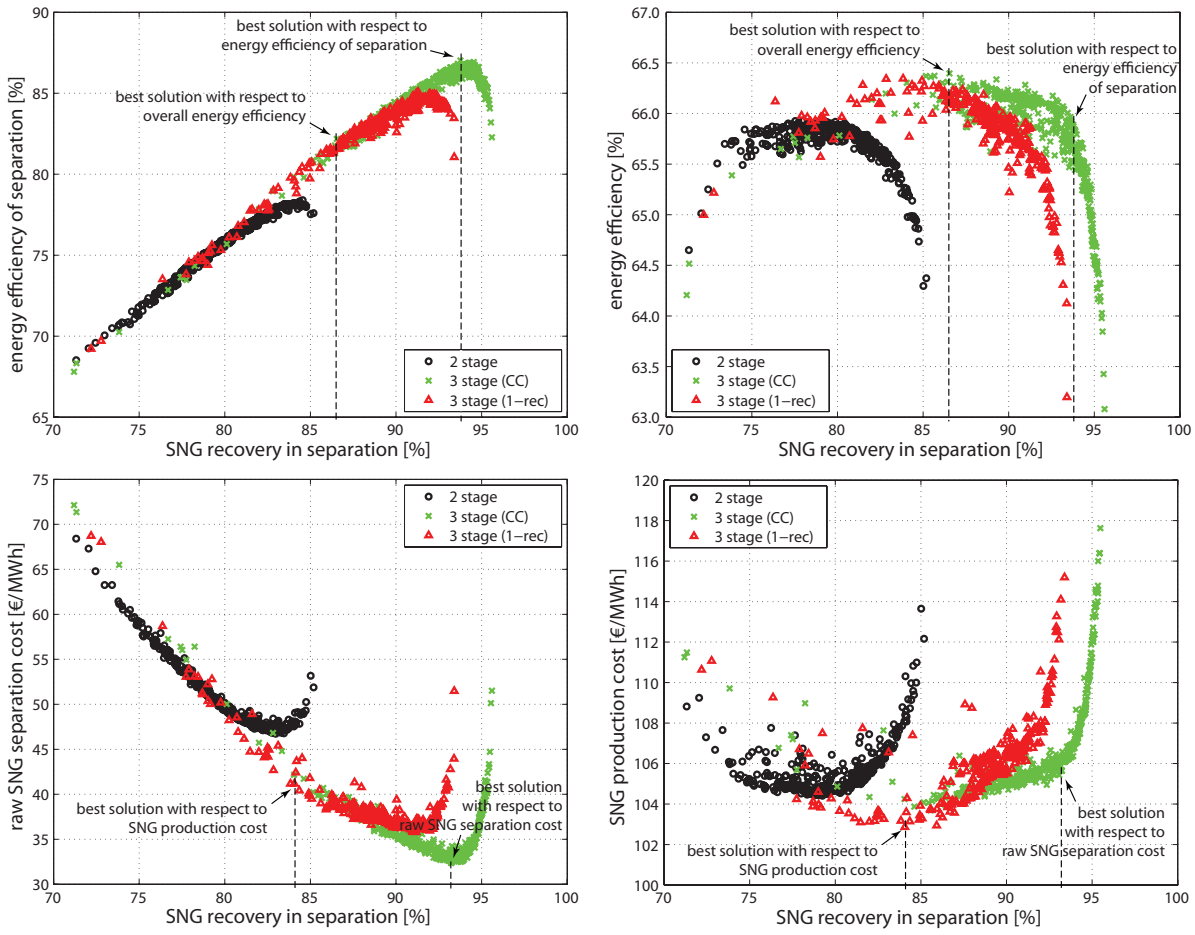

Figure 7: Energy efficiency (top) and production costs (bottom) of the separation system (left) and the total process (right).

		Optimal process with respect to:					
		separation system			overall plant		
		2s	3s, 1-rec	3s, CC	2s	3s, 1-rec	3s, CC
θ_1	-	0.28	0.32	0.57	0.46	0.39	0.38
θ_2	-	0.72	0.58	0.47	0.46	0.33	0.44
θ_3	-	-	0.48	0.55	-	0.34	0.38
p_{p_1}	bar	1.0	1.1	1.0	1.0	1.0	1.3
p_{p_2}	bar	1.0	3.8	2.1	1.0	2.2	2.9
p_{p_3}	bar	-	1.1	1.2	-	1.0	1.3
p_{f_1}	bar	15.5	11.7	12.2	16.6	14.8	11.0
p_{f_2}	bar	49.5	26.0	21.4	49.8	35.9	27.3
p_{f_3}	bar	-	49.4	47.0	-	44.5	42.0
$s_{in,2}$	-	-	0.94	1.00	-	0.02	0.07
r_{SNG}	%	84.5	91.3	93.8	78.0	83.8	86.5
e^{sep}_{spec}	$kW_{el}/MW_{th,in}$	78.5	72.9	77.4	49.1	50.7	53.1
C^{sep}_I	M€	6.7	7.0	6.7	4.4	4.6	5.9
$\tilde{c}_{CO2,p}$	%	79.9	85.0	86.9	75.8	79.7	81.5
$\tilde{c}_{H2,p}$	%	9.9	10.2	10.4	9.2	9.5	9.8
$\tilde{c}_{CH4,p}$	%	9.9	4.6	2.5	14.6	10.5	8.5
A	m^2	6024	7317	6537	3911	4129	6490
C^{sep}_P	€/MWh	49.1	36.7	33.2	52.2	41.2	38.9
$\Delta h^0_{wood,dry}\dot{m}^+_{wood,dry}$	MW	20.0	20.0	20.0	20.0	20.0	20.0
$\Delta h^0_{crudeSNG}\dot{m}^+_{crudeSNG}$	MW	15.0	14.0	13.7	16.1	15.1	14.7
$\Delta h^0_{SNG}\dot{m}^-_{SNG}$	MW	12.7	12.8	12.9	12.6	12.7	12.7
$\dot{E}^{sep,+}$	MW	1.18	1.02	1.06	0.79	0.77	0.78
$\dot{E}^-$	MW	0.28	0.35	0.31	0.63	0.59	0.55
ε^{sep}	%	78.4	85.1	87.0	74.4	79.8	82.2
ε	%	64.9	65.9	65.9	65.9	66.3	66.4
C_I	M€	32.5	32.2	31.7	30.9	30.3	31.4
C_P	€/MWh	110.8	108.2	107.6	104.5	103.2	105.0

Table 8: Decision variables, objectives, performance indicators and key properties of best designs with respect to energy efficiency.

		Optimal process with respect to:					
		separation system			overall plant		
		2s	3s, 1-rec	3s, CC	2s	3s, 1-rec	3s, CC
θ_1	-	0.35	0.40	0.56	0.44	0.39	0.45
θ_2	-	0.62	0.58	0.52	0.48	0.40	0.44
θ_3	-	-	0.39	0.46	-	0.24	0.32
p_{p1}	bar	1.0	1.1	1.0	1.0	1.0	1.1
p_{p2}	bar	1.0	3.8	3.0	1.1	2.2	4.3
p_{p3}	bar	-	1.1	1.1	-	1.4	1.8
p_{f1}	bar	17.4	20.1	12.1	22.8	24.4	23.5
p_{f2}	bar	49.9	49.7	35.9	47.7	49.0	49.5
p_{f3}	bar	-	49.9	50.0	-	49.0	50.0
$s_{in,2}$	-	-	0.94	0.98	-	0.00	0.21
r_{SNG}	%	83.0	91.2	93.2	79.3	84.1	85.6
e^{sep}_{spec}	$kW_{el}/MW_{th,in}$	63.9	80.2	76.9	54.2	55.9	60.0
C^{sep}_I	M€	5.3	5.4	5.7	4.3	4.1	4.6
$\tilde{c}_{CO2,p}$	%	78.9	85.0	86.6	76.6	79.9	80.8
$\tilde{c}_{H2,p}$	%	9.7	10.1	10.3	9.3	9.4	9.7
$\tilde{c}_{CH4,p}$	%	11.1	4.8	3.0	13.7	10.4	9.2
A	m^2	4423	3712	4675	3304	2928	3466
C^{sep}_P	€/MWh	46.7	35.8	32.4	50.6	41.2	40.0
$\Delta h^0_{wood,dry}\dot{m}^+_{wood,dry}$	MW	20.0	20.0	20.0	20.0	20.0	20.0
$\Delta h^0_{crudeSNG}\dot{m}^+_{crudeSNG}$	MW	15.3	14.1	13.8	15.9	15.1	14.9
$\Delta h^0_{SNG}\dot{m}^-_{SNG}$	MW	12.7	12.8	12.9	12.6	12.7	12.7
$\dot{E}^{sep,+}$	MW	0.98	1.13	1.06	0.86	0.84	0.89
$\dot{E}^-$	MW	0.45	0.32	0.35	0.59	0.56	0.52
ε^{sep}	%	78.0	84.4	86.6	75.2	79.6	80.7
ε	%	65.6	65.7	66.0	65.9	66.2	66.2
C_I	M€	31.2	30.6	30.7	30.6	29.9	30.2
C_P	€/MWh	106.5	106.1	105.6	104.4	102.9	103.7

Table 9: Decision variables, objectives, performance indicators and key properties of best designs with respect to production cost.

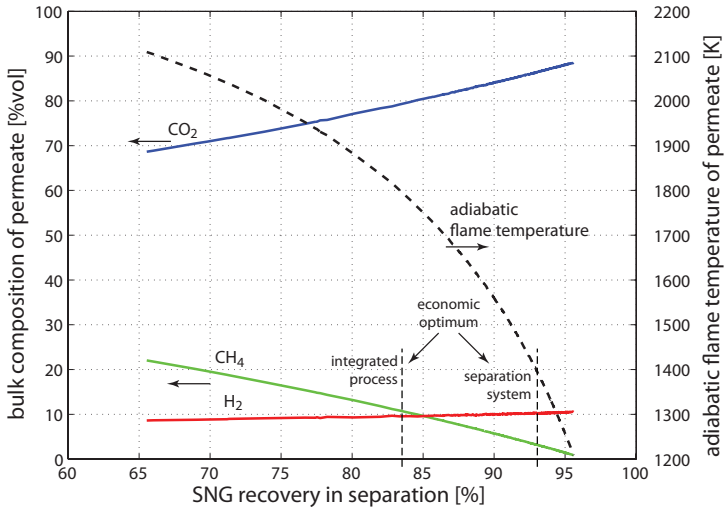

Figure 8: Molar composition and adiabatic flame temperature of the permeate stream.

energy content of the producer gas is directly used as utility, 11.0% is lost as methanation reaction heat, 3.5% is used as utility in the form of depleted membrane permeate and 65.6% is present as final product. At 85% recovery, only 11.7% of the producer gas is withdrawn from the process stream, and the share of the depleted membrane permeate used as utility is close to 50%. Although this results in a decreasing utility demand from 23.4% to 23.1% due to the more advantageous combustion properties of the permeate, a slight decrease to 64.7% of final product is caused by an increase of the methanation reaction heat loss to 12.2%. At about 75%, the complete heat demand of the gasifier is satisfied by the membrane permeate, and no more savings of producer gas can be obtained below.

5.4 Process optimisation for CO_2 capture

In the previous sections, the design of the separation system is only focussed on the upgrading of the main product to grid quality and the CO_2-rich stream is considered as waste. In order to prevent the emission of the remaining highly active greenhouse gas CH_4 to the atmosphere, the final membrane permeate is completely oxidised. In the most economic designs, the purity of the CO_2 in this stream does thereby not exceed 80%, which allows for recovering its heating value at a sufficiently high temperature to be useful for the process.

A priori, the elevated amount of CO_2 in the bulk composition of the crude SNG encourages for producing not only SNG, but also recovering the CO_2 as a by-product. In case of SNG production from biomass, applying carbon capture and storage (CCS) would thereby turn the process into an atmospheric CO_2-sink if the resource is exploited in a sustainable way (i.e. no deforestation and limited impact from biomass processing). In fact, the complete oxidation of biogenic carbon does not produce net emissions of CO_2, since it has previously been extracted through photosynthesis during plant growth and the carbon cycle is closed. When the reemission of CO_2 is partly prevented by its capture at the conversion plant and sequestration, the net balance of emitted greenhouse gases becomes indeed negative considering the entire life cycle of the product.

In order to facilitate approaching a typical purity requirement of 95% for CCS, preliminary calculations suggest to complete the membrane process layout with an enriching stage of the same material. As shown in Figures 5b-d, the retentate of this additional stage (E1) is thereby not recycled to the stripping section (stage 1), but withdrawn from the membrane system. The separation of the main product is thus not additionally loaded by diluting the feed, and the heating value of the low-value retentate of stage E1 can be used as utility with more advantageous fuel properties than the originally used permeate from stage 1. To attain the purity requirement for sequestering the permeate from E1, two strategies are envisaged.

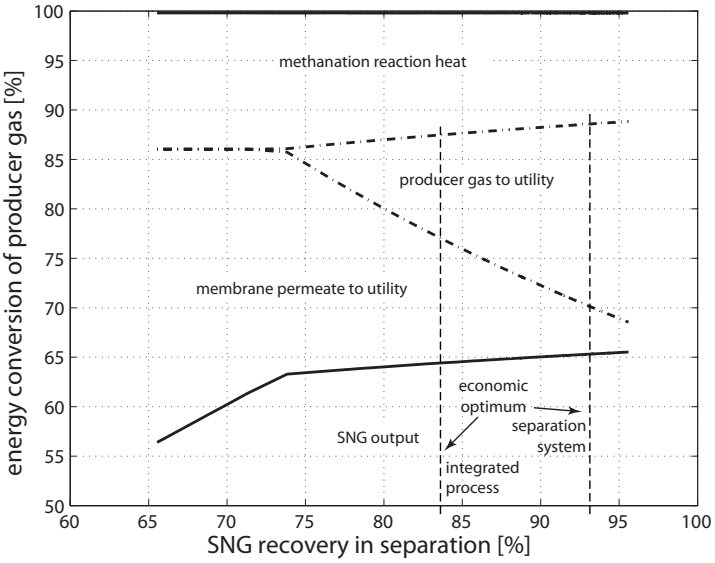

Figure 9: Conversion of the chemical energy in the producer gas through the system.

On the one hand, it could be directly brought to sufficient purity and captured, including the residual H_2, CH_4 and minor amounts of CO and N_2. Alternatively, the residual H_2, CH_4 and CO may be completely oxidised to CO_2, in which case the captured CO_2 is only accompanied by 5%vol of inert N_2. As shown on Figure 3, this can be done by catalytically combusting the E1-permeate with enriched air, for which the required oxygen is obtained through electrolysis. The by-produced H_2 can thereby be fed to the methanation and results in an increase of the SNG yield (Gassner and Maréchal, 2008).

In order to find optimal process configurations for CCS, the multi-objective optimisation strategy is applied to the most promising layouts. As objectives, the amount of captured carbon per total carbon in the biomass feed (hereafter termed as carbon capture ratio) is maximised while the production cost defined in Eq. 11 for SNG including CCS is minimised. Like in Section 5.3, base case conditions for the crude gas production are assumed and the same decision variables for the stripping section are considered (Table 7). Figure 10 shows the computed impact of the carbon capture on the production cost of SNG and the process efficiency, as well as the specific power consumption and cost for the recovery of 95% pure CO_2 at atmospheric pressure and temperature. In Table 10, the operating conditions and performance of some selected process designs that are highlighted in Figure 10 are given.

For small amounts of captured carbon, direct capture without catalytic combustion proves to be better. Since no additional equipment for electrolysis and catalytic combustion is needed and only additional membrane surface and compression power is required, the production cost increases and the energy efficiency decreases almost continuously from the best solution without capture. When the capture ratio reaches about 15%, it becomes more and more difficult to attain the purity requirement, the penalties on cost and efficiency increase considerably and direct capture gets suboptimal. At higher capture ratios, catalytic combustion with enriched air becomes profitable due to the less strict purity requirement of the permeate and the advantage of recovering its heating value. For this setup, the cost and efficiency penalty increases considerably from about 30% onwards. At this ratio, the flame temperature of enriched air combustion also begins to exceed the pinch point of the process and the stream must be used as a heat service for the gasification. The gasifier design would thus become more complex since heat needs to be supplied from two physically separated combustion chambers (one with normal, one with enriched air). At this technological barrier, 30% of carbon contained in the biomass is captured, 35% of the carbon leaves the process as SNG and 35% is released to the environment in the on-site flue gas.

If the specific cost and power consumption per ton of CO_2 is considered, the optimal carbon capture ratio lies around 15% for direct capture and at 25-30% for capture after catalytic combustion. At these

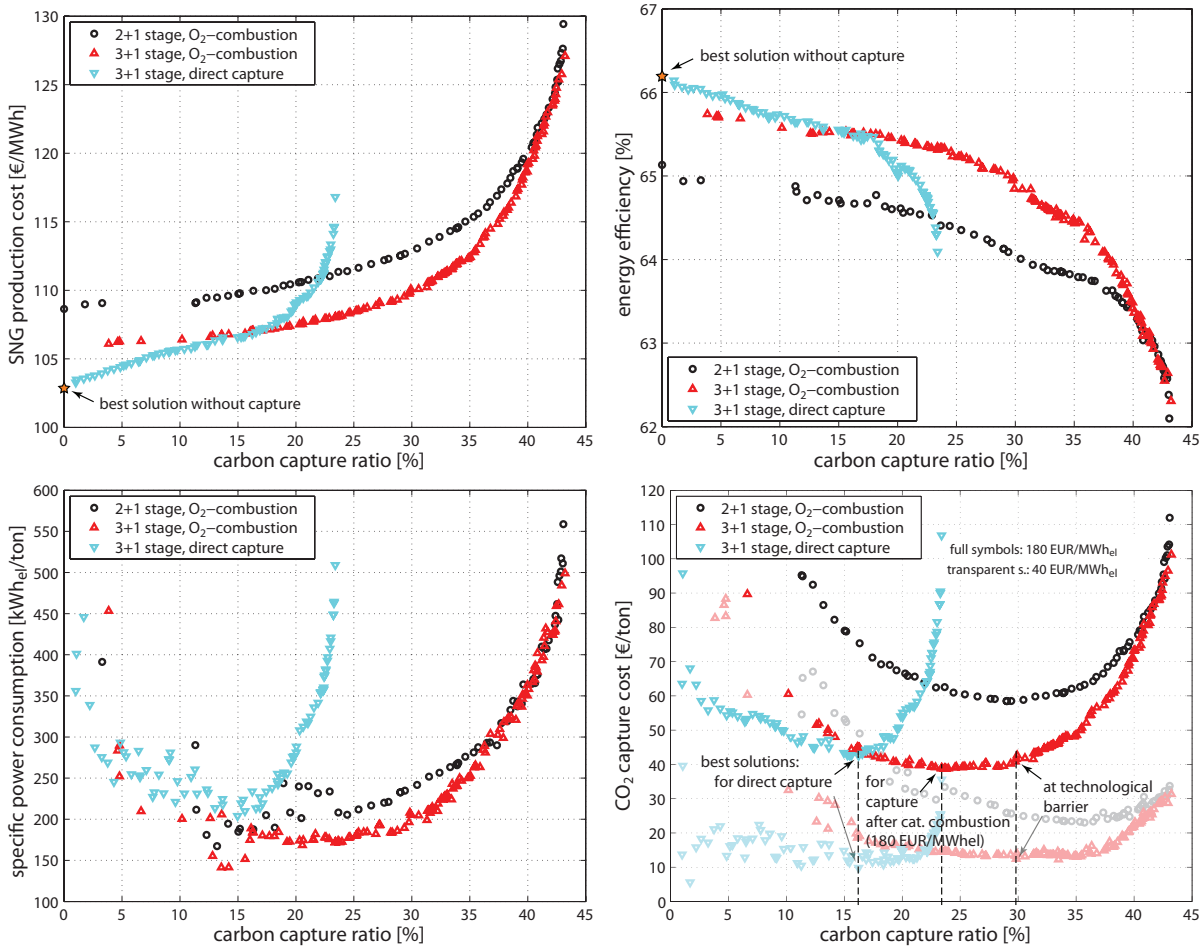

Figure 10: Pareto-optimal solutions for CO_2-capture (top, right) and its impact on the process efficiency (top, left). Specific electricity consumption (bottom, left) and relative cost (bottom, right) of capture for two different electricity prices.

Mode of capture		none	direct	catalytic combustion with enriched air	
Selection criteria		min. C_P	min. C_{CO2}	min. C_{CO2}	techn. barrier
θ_1	-	0.39	0.35	0.41	0.37
θ_2	-	0.40	0.43	0.34	0.35
θ_3	-	0.24	0.28	0.27	0.36
θ_{E1}	-	-	0.35	0.48	0.63
p_{p_1}	bar	1.0	2.2	3.4	3.6
p_{p_2}	bar	2.2	2.4	2.1	3.0
p_{p_3}	bar	1.4	1.1	1.1	1.3
$p_{p_{E1}}$	bar	-	1.1	1.1	1.2
p_{f_1}	bar	24.4	27.0	33.9	32.8
p_{f_2}	bar	49.0	49.3	47.1	45.2
p_{f_3}	bar	49.0	49.9	49.1	48.6
$p_{f_{E1}}$	bar	-	12.1	6.7	13.8
$s_{in,2}$	-	0.00	0.02	0.00	0.01
$s_{p1,E1}$	-	-	0.00	0.00	0.00
r_{SNG}	%	84.1	85.5	82.2	83.8
e^{sep}_{spec}	$kW_{el}/MW_{th,in}$	55.9	71.2	63.7	69.4
C^{sep}_I	M€	4.1	5.0	4.9	5.1
$\tilde{c}_{CO2,p}$	%	79.9	95.0	93.6	93.0
$\tilde{c}_{H2,p}$	%	9.4	4.3	5.1	5.6
$\tilde{c}_{CH4,p}$	%	10.4	0.7	1.3	1.3
A	m^2	2928	3253	3516	3532
C^{sep}_P	€/MWh	41.2	43.0	47.4	46.0
$\Delta h^0_{wood}\dot{m}^+_{wood}$	MW	20.0	20.0	20.0	20.0
$\Delta h^0_{crudeSNG}\dot{m}^+_{crudeSNG}$	MW	15.1	15.0	15.6	15.4
$\Delta h^0_{SNG}\dot{m}^-_{SNG}$	MW	12.7	12.8	12.8	12.9
$\dot{E}^{sep,-}$	MW	0.84	1.07	0.99	1.07
$\dot{E}^-$	MW	0.56	0.29	0.27	0.11
ε^{sep}	%	79.6	79.8	77.3	78.3
ε	%	66.2	65.5	65.3	65.0
C_I	M€	29.9	30.6	31.2	31.4
C_P	€/MWh	102.9	106.8	108.0	109.9
carbon capture ratio	%	-	16.2	23.4	29.8
carbon in SNG	%	34.7	35.0	35.0	35.3
carbon emitted on site	%	65.3	48.8	41.6	34.9
$C^{electrolysis\ \&\ cat.\ comb.}_I$	k€	-	-	189	302
rel. increase of C_I	%	-	2.4	4.3	5.0
spec. power for CCS	kWh_{el}/ton_{CO2}	-	234	172	208
C_{CO2} (180 €/MWh_{el})	€/ton_{CO2}	-	42.5	38.8	41.6
C_{CO2} (40 €/MWh_{el})	€/ton_{CO2}	-	9.8	14.7	12.5

Table 10: Decision variables, objectives, performance indicators and key parameters of selected designs for CCS in comparison with the reference solution without capture.

ratios, the net specific power consumption for CO_2 purification is in the order of 200 kWh/ton, and the process efficiency is decreased by 0.5-1%. The cost of capture is therefore strongly dependent on the cost of electricity. If a price of 180 €/MWh for green electricity is considered, the share of expenses for electricity contributes to more than 80% at the optimal capture ratios, the rest being related to the additional investment. If typical electricity generation costs of 40 €/MWh for new coal and natural gas power plants without CCS are assumed (Meth et al., 2005), the cost of captured – and avoided – CO_2 drops from 40 €/ton to below 15 €/ton. This value is considerably lower than the ones compiled by Meth et al. (2005) for CCS from fossil fuel power plants. It is therefore potentially more economic to do CCS via an SNG plant that doing the capture at the power plants itself, and trading CO_2 certificates could be used as a way to increase the profitability of the SNG production.

6 Conclusions

By implementing a thermo-economic model for multicomponent membrane gas separation in a process model for SNG production, different design approaches for SNG upgrading to grid quality have been compared. Using multi-objective optimisation, it has been shown that the resulting system design and performance depends markedly on the level of process integration that is implemented. When the interactions between the separation system and the reactive parts of the process are disregarded and only the isolated performance of the separation system is considered, the size, cost and electricity consumption of the separation are significantly exaggerated. When the process integration is included in the design problem, advantage is taken from using depleted gas from the separation as utility and less product recovery is required. For the considered membrane properties and design constraints, a globally optimal system recovers only about 84% instead of 93% of the crude SNG and satisfies about 50% of the heat demand with depleted membrane permeate.

Finally, different strategies for simultaneously purifying the by-produced CO_2 to fulfil the requirements for long-term storage have been investigated. It has been shown that completely oxidising the residual CH_4, H_2 and CO in a catalytic combustion with enriched air from electrolysis is promising. This is because less effort must been put into the gas separation, the heating value of the residues is recovered and the by-produced hydrogen increases the SNG yield. The cost of captured and avoided CO_2 is strongly dependent on the cost of electricity and lies in the range of 15 to 40€/ton. This value is lower than the cost for avoiding CO_2 at a fossil power plant. Capturing CO_2 at the SNG plant using electricity from a centralised power plant is thus potentially more economic than investing in an end-of-pipe capture at the power plant.

Acknowledgements

The authors acknowledge funding provided by the Competence Centre for Energy and Mobility (CCEM-CH), Erdgas Ostschweiz AG, Gasverbund Mittelland AG and Gaznat SA (all Switzerland).

A Pettersen and Lien's design model

Using the Paterson approximation to the logarithmic mean, Pettersen and Lien (1994) have formulated their simplified multicomponent design model in a quadratic form, from which the permeate molar fraction $\tilde{c}_{i,p}$ of a substance i is explicitly calculated by:

$$\tilde{c}_{i,p} = \frac{-b_i + \sqrt{b_i^2 - 4a_i c_i}}{2a_i} \tag{19}$$

were the parameters a_i, b_i and c_i are combinations of the ratio of absolute pressures Π_r, the molar stage cut θ, a dimensionless permeation factor R_i and the feed fraction $\tilde{c}_{i,f}$:

$$a_i = \frac{\Pi_r}{3}\left(\frac{2\theta}{R_i} - \Pi_r\right) + \left(\frac{\theta}{R_i}\right)^2 + \frac{\theta}{3(1-\theta)}\left(\frac{\theta}{R_i} + \frac{\theta}{12(1-\theta)} - \Pi_r\right) \tag{20}$$

$$b_i = \frac{\tilde{c}_{i,f}}{3}\left(1 + \frac{1}{1-\theta}\right)\left(\Pi_r - \frac{\theta}{R_i}\right) + \frac{\theta\tilde{c}_{i,f}}{18(1-\theta)}\left(7 - \frac{1}{1-\theta}\right) \tag{21}$$

$$c_i = \left(\frac{\tilde{c}_{i,f}}{6(1-\theta)}\right)^2 (\theta^2 + 12\theta - 12) \tag{22}$$

with Π_r, θ and R_i defined as:

$$\Pi_r = \frac{p_p}{p_f} \tag{23}$$

$$\theta = \frac{\dot{n}_p}{\dot{n}_f} \tag{24}$$

$$R_i = \frac{AP_i p_f}{\delta \dot{n}_f} \tag{25}$$

References

Adhikari, S., Fernando, S., 2006. Hydrogen membrane separation techniques. Industrial and Engineering Chemistry Research 45 (3), 875–881.

Baker, R., 2002. Future directions of membrane gas separation technology. Industrial and Engineering Chemistry Research 41 (6), 1393–1411.

Bart, H.-J., von Gemmingen, U., 2009. Adsorption. In: Ullmann's encyclopedia of industrial chemistry, 7th Edition. Wiley-VCH.

Belsim SA, last visited 04/2009. Vali IV. www.belsim.com.

Bhide, B., Stern, S., 1993a. Membrane processes for the removal of acid gases from natural gas. I. Process configurations and optimization of operating conditions. Journal of Membrane Science 81, 209–237.

Bhide, B., Stern, S., 1993b. Membrane processes for the removal of acid gases from natural gas. II. Effects of operating conditions, economic parameters, and membrane properties. Journal of Membrane Science 81 (3), 239–252.

Budd, P., Msayib, K., Tattershall, C., Ghanem, B., Reynolds, K., McKeown, N., Fritsch, D., 2005. Gas separation membranes from polymers of intrinsic microporosity. Journal of Membrane Science 251 (1-2), 263–269.

Cao, C., Chung, T.-S., Liu, Y., Wang, R., Pramoda, K., 2003. Chemical cross-linking modification of 6fda-2,6-dat hollow fiber membranes for natural gas separation. Journal of Membrane Science 216 (1-2), 257–268.

Cavenati, S., Grande, C., Rodrigues, A., 2006. Removal of carbon dioxide from natural gas by vacuum pressure swing adsorption. Energy and Fuels 20 (6), 2648–2659.

Cecopieri-Gomez, M., Palacios-Alquisira, J., Dominguez, J., 2007. On the limits of gas separation in co2/ch4, n2/ch4 and co2/n2 binary mixtures using polyimide membranes. Journal of Membrane Science 293 (1-2), 53–65.

Chung, T., Jiang, L., Li, Y., Kulprathipanja, S., 2007. Mixed matrix membranes (MMMs) comprising organic polymers with dispersed inorganic fillers for gas separation. Progress in Polymer Science 32 (4), 483–507.

Doong, S., Yang, R., 1987. A comparison of gas separation performance by different pressure swing adsorption cycles. Chemical Engineering Communications 54 (1-6), 61–71.

Ducreux, O., Lavigne, C., Nedez, C., 2006. Air and gas drying with activated alumina. www.axens.net, Axens IFP Group Technologies.

Duret, A., Friedli, C., Maréchal, F., 2005. Process design of Synthetic Natural Gas (SNG) production using wood gasification. Journal of Cleaner Production 13, 1434–1446.

Gandhidasan, P., 2003. Parametric analysis of natural gas dehydration by a triethylene glycol solution. Energy Sources 25 (3), 189–201.

Gandhidasan, P., Al-Farayedhi, A., Al-Mubarak, A., 2001. Dehydration of natural gas using solid desiccants. Energy 26 (9), 855–868.

Gassner, M., Maréchal, F., 2008. Thermo-economic optimisation of the integration of electrolysis in synthetical natural gas production from wood. Energy 33, 189–198.

Gassner, M., Maréchal, F., 2009a. Methodology for the optimal thermo-economic, multi-objective design of thermochemical fuel production from biomass. Computers and Chemical Engineering 33, 769–781.

Gassner, M., Maréchal, F., 2009b. Thermo-economic process model for thermochemical production of synthetic natural gas (SNG) from lignocellulosic biomass. Submitted in revised form to Biomass and Bioenergy , .

Gassner, M., Maréchal, F., 2009c. Thermodynamic comparison of the FICFB and Viking gasification concepts. Energy, in press.

Girardin, L., Maréchal, F., Tromeur, P., 2006. Methodology for the design of industrial hydrogen networks and the optimal placement of purification units using multi-objective optimisation techniques. In: 16th European Symposium on Computer Aided Process Engineering and 9th International Symposium on Process Systems Engineering.

Hagg, M., Lie, J., Lindbrathen, A., 2003. Carbon molecular sieve membranes - a promising alternative for selected industrial applications. Advanced Membrane Technology 984, 329–345.

Heyne, S., Thunman, H., Harvey, S., 2008. Integration aspects for synthetic natural gas production from biomass based on a novel indirect gasification concept. In: PRES 2008, 11th Conference on Process Integration, Modelling and Optimisation for Energy Saving and Pollution Reduction. Prague.

Hofbauer, H., Rauch, R., Löeffler, G., Kaiser, S., Fercher, E., Tremmel, H., 2002. Six years experience with the FICFB-gasification process. In: Proceedings of the 12th European Conference and Technology Exhibition on Biomass for Energy, Industry and Climate Protection. Amsterdam, Netherlands.

Hogsett, J., Mazur, W., 1983. Estimate membrane system area. Hydrocarbon Processing 62 (8), 52–54.

Hradil, J., V., K., Hrabanek, P., Bernauer, B., Kocirik, M., 2004. Heterogeneous membranes based on polymeric adsorbents for separation of small molecules. Reactive and Functional Polymers 61 (3), 57–68.

Hwang, S.-T., Kammermeyer, K., 1975. Membranes in separation. Vol. 7 of Techniques of chemistry. Wiley, New York.

Ismail, A., David, L., 2001. A review on the latest development of carbon membranes for gas separation. Journal of Membrane Science 193 (1), 1–18.

Kapoor, A., Yang, R., 1989. Kinetic separation of methane carbon-dioxide mixture by adsorption on molecular-sieve carbon. Chemical Engineering Science 44 (8), 1723–1733.

Kim, M.-B., Bae, Y.-S., Choi, D.-K., Lee, C.-H., 2006. Kinetic separation of landfill gas by a two-bed pressure swing adsorption process packed with carbon molecular sieve: Nonisothermal operation. Industrial and Engineering Chemistry Research 14 (14), 5050–5058.

Knaebel, K., Reinhold, H., 2003. Landfill gas. From rubbish to resource. Adsorption – Journal of the International Adsorption Society 9 (1), 87–94.

Koros, W., Mahajan, R., 2000. Pushing the limits on possibilities for large scale gas separation: Which strategies? Journal of Membrane Science 175 (2), 181–196.

Li, S., Martinek, J., Falconer, J., Noble, R., Gardner, T., 2005. High-pressure co2/ch4 separation using sapo-34 membranes. Industrial and Engineering Chemistry Research 44 (9), 3220–3228.

Liu, L., Chen, Y., Kang, Y., Deng, M., 2001. An industrial scale dehydration process for natural gas involving membranes. Chemical Engineering and Technology 24 (10), 1045–1048.

Luterbacher, J., Fröling, M., Vogel, F., Maréchal, F., Tester, J. W., 2009. Hydrothermal gasification of waste biomass: Process design and life cycle assessment. Environmental Science and Technology 43, 1578–1583.

Meth, B., Davidson, O., de Coninck, H., Loos, M., Meyer, L. (Eds.), 2005. IPCC special report on carbon dioxide capture and storage. IPCC.

Mozaffarian, M., Zwart, R. W. R., 2003. Feasibility of biomass/waste-related SNG production technologies. Tech. rep., ECN, Petten.

Pettersen, T., Lien, K., 1994. A new robust design model for gas separating membrane modules, based on analogy with counter-current heat exchangers. Computers and Chemical Engineering 18 (5), 427–439.

Phair, J., Badwal, S., 2006. Materials for separation membranes in hydrogen and oxygen production and future power generation. Science and Technology of Advanced Materials 7, 792–805.

Qi, R., Henson, M., 1998. Optimization-based design of spiral-wound membrane systems for CO2/CH4 separations. Separation and Purification Technology 13 (3), 209–225.

Rauch, R., written around 2004. Stromerzeugung aus Biomasse durch Wasserdampfvergasung. Tech. rep., Institut für Verfahrens-, Brennstoff- und Umwelttechnik, TU Wien, www.ficfb.at, last visited 04/2009.

Rautenbach, R., Dahm, W., 1985. The separation of multicomponent mixtures by gas permeation. Chemical Engineering and Processing 19 (4), 211–219.

Ritter, J., Ebner, A., 2007. State-of-the-art adsorption and membrane separation processes for hydrogen production in the chemical and petrochemical industries. Separation Science and Technology 42 (6), 1123–1193.

Robeson, L., 1991. Correlation of separation factor versus permeability for polymeric membranes. Journal of Membrane Science 62 (2), 165–185.

Sircar, S., 1988. Separation of methane and carbon-dioxide gas-mixtures by pressure swing adsorption. Separation Science and Technology 23 (6-7), 519–529.

Spillman, R., 1989. Economics of gas separation membranes. Chemical Engineering Progress 85 (1), 41–62.

Staudt-Bickel, C., Koros, W., 1999. Improvement of CO2/CH4 separation characteristics of polyimides by chemical crosslinking. Journal of Membrane Science 155 (1), 145–154.

Stucki, S., 2005. Projet bois–methane. Rapport sur la clôture de la phase 1 du projet: Preuve de la faisabilité technique à l'échelle du laboratoire. Tech. rep., PSI, Villigen, Switzerland.

SVGW, 2008. G13, Richtlinien für die Einspeisung von Biogas ins Erdgasnetz. Zürich.

Turton, R., Bailie, R. C., Whiting, W. B., Shaeiwitz, J. A., 1998. Analysis, synthesis, and design of chemical processes. Prentice Hall, New York.

Ulrich, G. D., Vasudevan, P. T., 2004. Chemical engineering process design and economics. A practical guide, 2nd Edition. Process publishing, New Hampshire.

Urban, W., Girod, K., Lohmann, H., 2008. Technologien und Kosten der Biogasaufbereitung und Einspeisung in das Erdgasnetz. Ergebnisse der Markterhebung 2007-2008. Tech. rep., Fraunhofer-Institut für Umwelt-, Sicherheits- und Energietechnik.

Waldron, W., Sircar, S., 2000. Parametric study of a pressure swing adsorption process. Adsorption – Journal of the International Adsorption Society 6 (2), 179–188.

Weller, S., Steiner, W. A., 1950. Separation of gases by fractional permeation through membranes. Journal of Applied Physics 21, 279–283.

Zou, J., Ho, W., 2006. CO2-selective polymeric membranes containing amines in crosslinked poly(vinyl alcohol). Journal of Membrane Science 286 (1-2), 310–321.